Bioresource Technology 319 (2021) 124118

Contents lists available at ScienceDirect

Bioresource Technology

journal homepage: www.elsevier.com/locate/biortech

Effect of proton pump inhibitor on microbial community, function, and kinetics in anaerobic digestion with ammonia stress

Dawei Yu [a,b,c,d], Qingqing Zhang [a,b,e], Bram De Jaegher [d], Jibao Liu [a,b,c], Qianwen Sui [a,b,c], Xiang Zheng [e,*], Yuansong Wei [a,b,c,*]

[a] State Key Joint Laboratory of Environmental Simulation and Pollution Control, Research Center for Eco-Environmental Sciences, Chinese Academy of Sciences, Beijing, China
[b] Department of Water Pollution Control Technology, Research Center for Eco-Environmental Sciences, Chinese Academy of Sciences, Beijing 100085, China
[c] University of Chinese Academy of Sciences, Beijing 100049, China
[d] BIOMATH, Department of Data Analysis and Mathematical Modelling, Ghent University, Coupure Links 653, Ghent 9000, Belgium
[e] School of Environment & Natural Resources, Renmin University of China, Beijing 100872, China

HIGHLIGHTS

- The proton pump inhibitor mitigated ammonia inhibition by the proton mechanism.
- Metabolic pathways of acetate compared at different dosages of proton pump inhibitor.
- Gompertz and Gaussian processes modeled deterministic kinetic and random effect.
- The proton pump mechanism of ammonia inhibition was refined with metagenomics.
- PPI dose showed potential in investigating molecular mechanism of ammonia inhibition.

GRAPHICAL ABSTRACT

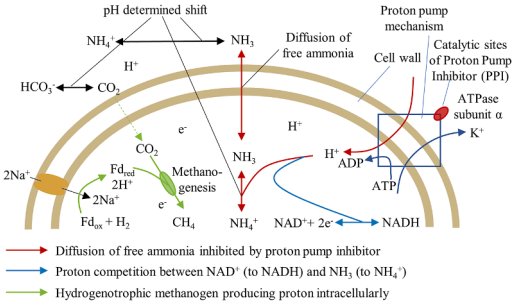

ARTICLE INFO

Keywords:
Methane
Ammonia
Proton pump
Kinetic
Anaerobic digestion

ABSTRACT

The proton pump is a convincing mechanism for ammonia inhibition in anaerobic digestion, which explained how the ammonia accumulated intercellularly due to diffusion of free ammonia. Proton pump inhibitor (PPI) was dosed for mitigating the accumulation in anaerobic digestion with ammonia stress, with respect to kinetics. Results show PPI inhibited β-oxidation of fatty acids by targeting ATPase in anaerobic digestion with ammonia stress. Alternatively, PPI stimulated syntrophic acetate oxidization. Random forest located key genera as syntrophic consortia. Methane increased 18.72 ± 7.39% with 20 mg/L PPI at the first peak, consistent with microbial results. The deterministic Gompertz kinetics and stochastic Gaussian processes contributed 97.63 ± 8.93% and 2.37 ± 8.93% in accumulated methane production, respectively. Thus, the use of PPI for anaerobic digestion allowed mitigate ammonia inhibition based on the mechanism of proton pump, facilitate intercellularly ammonia accumulation, stimulate syntrophic consortia, and eliminate uncertainty of process failure, which resulted in efficient methane production under ammonia stress.

* Corresponding authors at: State Key Joint Laboratory of Environmental Simulation and Pollution Control, Research Center for Eco-Environmental Sciences, Chinese Academy of Sciences, Beijing, China (Y. Wei).
E-mail addresses: zhengxiang7825@163.com (X. Zheng), yswei@rcees.ac.cn (Y. Wei).

https://doi.org/10.1016/j.biortech.2020.124118
Received 19 August 2020; Received in revised form 8 September 2020; Accepted 9 September 2020
Available online 15 September 2020

1. Introduction

Anaerobic digestion recovers energy from wastewater and organic waste, produced over 4.3×10^8 m^3 (i.e., 43 bcm) biogas in 2018, as 7.8% of renewable energies production in Europe. The two key inhibitors of anaerobic digestion facilities identified as acidification (bcm from food waste) and ammonia inhibition (43 bcm/y from manure), which all directly linked with proton conditions (Fuchs et al., 2018). Proton also participated in interspecies hydrogen transfer of electron by electron released from hydrogenases (Wu et al., 2020).

Proton pump played a significant role in intracellular pH regulation. The role of the plasma membrane, ion channel (e.g., Na^+/K^+-ATPase, Ca^{2+} transport ATPase), and H^+-ATPases were intensively investigated. There are several critical types: F-type ATP synthase / ATPase in bacteria and inner membranes, V-type ATPase in plants and fungi (Mulkidjanian et al., 2007), and P-type ATPase in archaea and eukarya (Bult et al., 1996). The intracellular pH of bacteria and archaea were therefore regulated if explored acidification risk. The regulation impacted methanogenesis by ion exchanges/trace elements and ATP energy processes. The proton pump played an essential role in the intracellular accumulation of NH_4^+, especially in methanogens (Jiang et al., 2019). Methanogens loss cytoplasmic ion through ammonia exchange reaction in the ion-free ammonia solution, for example, K^+, Na^+, and Mg^{2+} (Sprott and Patel, 1986). Free ammonia (FAN) enters the plasma membrane due to gradient and competes for the intracellular proton with enzymes, e.g., NAD from NADH (Wang et al., 2015). The proton pump must work harder to maintaining intracellular pH, meanwhile exchange K^+ out and cost ATP energy. The extra protons formed NH_4^+ with FAN and accumulated (Jiang et al., 2019). The intracellular accumulation of NH_4^+ stopped when FAN balanced between intracellular pH (~7.2 for most methanogens) and extracellular pH (7.0 ~ 8.5). The intracellular accumulation is also reversible with lower extracellular pH, which also relieved the inhibition of ammonia. The common source of acid and ammonia is protein as a substrate of anaerobic digestion.

Proton pump inhibitor (PPI) is a drug developed for maintaining gastric pH > 3 ~ 4, by targeting the gastric H^+/K^+-ATPase. The gastric H^+/K^+-ATPase is a non-covalently associated α, β-heterodimeric enzyme, where α subunit has the catalytic sites for ATP binding and phosphorylation, expressed from conserved sequences with P_2 type ATPases. The target binding site was a phosphorylation site observed at Asp386, a well-conserved in P-type ATPases (Shin and Kim, 2013). A sequence with very high homology to P-type H^+-ATPase has been identified in the genome of the archaeal *Methanococcus janashii* (Bult et al., 1996). The target phosphorylation site is well conserved in P-type ATPases of gastric and non-gastric H^+/K^+-ATPase α subunit.

The PPI trends to accumulate in acidic space of the plasma membrane of the stimulated cell (Shin et al., 2004). After accumulated and binding to the P-type ATPase, the PPI activates by low pH, to form the thiophilic drug that reacts with luminally accessed cysteines on the P-type ATPase. In test active pH 0–8.0, lower pH could activate the proton pump more quickly, and half-lives decrease from 6477 min to 1.4 min (Shin et al., 2004). The activated PPI is binding to the P-type ATPase by disulfide. The inhibition of the proton pump was linear with the bond of ATPase. The disulfide bond is weak on reductive cleavage, with half-lives of 12 – 20 h (Shin and Sachs, 2004). There will be no permanent damage after the initial period of inhibition on the existing proton pump and no further impacts on the new proton pump. If well targeted, the PPI could be promising in accelerate acclimation to ammonia by mitigating intracellular accumulation of NH_4^+ and the initial inhibition.

Therefore, the effects of PPI on anaerobic digestion under ammonia stress were tested by methanogenic kinetics and physicochemical performance, with special attention on the evolution of the microbial community and their functions. Meanwhile, random effects also considered avoiding bias.

2. Materials and methods

2.1. Proton pump inhibitor

The PPI was tested for its effects on the proton pump in anaerobic digestion. There are seven proton inhibitors, including Timoprazole, Picoprazole, Omeprazole, Lansoprazole, Pantoprazole, Rabeprazole, and finally, Tenatoprazole (Shin et al., 2004). Lansoprazole was selected for the intracellular FAN test, considering ion condition, site of reaction, and potential in archaea as eukaryote (Shin et al., 2004). The Omeprazole directly inhibits the last step of the proton pump by bonding with H^+/K^+-ATPase (Shin and Kim, 2013). Most PPI will be more active at lower pH values. These knowledge gaps limited the application of PPI in researches on the role of proton pump in intracellular FAN. In light of this knowledge, a PPI could help in understanding the role of the proton pump in intracellular FAN, and FAN's gradient across the cell wall especially. The Lansoprazole (CAS103577-45–3, Sigma-Aldrich, Germany) were dissolved in 0.1 $mol{\cdot}L^{-1}$ NaOH for the following use.

The effect of Lansoprazole on anaerobic digestion of tryptone was tested without active by acid before dose. The Lansoprazole could be active by acid at pH < 2 (30 min) before dosing to anaerobic digestion (Shin and Kim, 2013). The activation was not taken for maintaining enough dose during days of lag-phase time. Once fatty acid accumulated, the Lansoprazole should activate as a PPI. To the best of knowledge, this study is the first to demonstrate the effect of proton pump regulation in anaerobic digestion under ammonia stress. In light of the previous proton pump mechanism of ammonia intracellular accumulation (Jiang et al., 2019), the method proposed a novel approach of molecular level regulation of proton pump in anaerobic digestion under ammonia stress.

2.2. Experimental determination of apparent kinetic parameters

Tryptone contained 4.9% amino-N, which was used as a model protein source for methanogenesis kinetic test (Nielsen and Ahring, 2007). The tryptone was selected after preliminary experiments in glucose without ammonia stress. The PPI showed slightly inhibition on methane production in anaerobic digestion of glucose, which was reasonable due to PPI's potential impaction on interspecies hydrogen transfer. The tryptone was also selected for unrevealing evolution of community and functional roles during anaerobic digestion of protein, in light of previous works (Zhu et al., 2019). The tryptone solution was used as a substrate, its COD, ammonia, and pH were 16940 mg/L, 1000 mg/L, and 7.46.

The substrate was inoculated with an inoculum/substrate ratio at 0.77 $kgVS{\cdot}kgCOD^{-1}$. The inoculum was anaerobic digestion sludge collected from the Beijing Xiaohongmen Wastewater Treatment Plant Prior to inoculate, the sludge filtered with a sieve of 18 mesh and sampled for further analysis. The filtered sludge was used as inoculum, its COD, ammonia, pH, TS, and VS were 5662 mg/L, 2557 mg/L, 7.69, 5.08%, and 2.40%. Then the tryptone solution was inoculated with the inoculum. The inoculated substrate's COD, ammonia, and pH were 12371 mg/L, 1827 mg/L, and 8.13. The inoculated substrate subpackaged in 400 ml Serum bottles as 15 parallel tests. The tests grouped according to PPI doses into five groups: CK (0.00 mg/L), PP1 (1.00 mg/L), PP5 (5.00 mg/L), PP10 (10.00 mg/L), and PP20 (20.00 mg/L). The bottles sealed up with toppers equipped with 120 RPM stirrer and submerged in a 37 °C water bath after blowing nitrogen to remove oxygen, as mesophilic anaerobic digestion. The gas production absorbed by 3 mol/L NaOH solution to remove carbon dioxide, and measured by an online micro gas flowmeter to record daily methane production. Each bottle sampled at days 1, 10, and 33, i.e., start (D1), middle (D10), and end (D33). The test stopped after daily methane production lower than 2 ml in the last five days.

Maximal daily methane production ($mlCH_4/g/day$), methane yield ($mlCH_4/g/day$), and lag-phase time (day) were determined by the

Gompertz equation, to quantify the PPI's apparent kinetic impacts (eq. (1)).

$$AMP(t) = \mathrm{BMP} \cdot \exp(-\exp(R_m \cdot (\lambda - t) - 1)) \quad (1)$$

where, AMP, BMP, R_m, λ, and t refer to accumulated methane production (at time *t*), biochemical methane potential (BMP) ($mlCH_4/g$), and maximal daily methane production, and lag-phase time, respectively. The Residual Sum of Squares (RSS) and Root Mean Squared Error (RMSE) were reported (Strömberg et al., 2014). Residual errors of the Gompertz equation were also recorded for further analysis.

2.3. Gaussian Processes of the residual errors

Random effects in the residual errors of the Gompertz model were modeled by Gaussian Processes in machine learning, as the residual followed Gaussian distribution, i.e., Normal distribution. The Gaussian Processes beyond the determination of apparent kinetics were widely observed as random effects in residual errors of kinetic tests. Progress in machine learning allowed the random effects learned as a stochastic process by the Gaussian Processes method. The Gaussian Processes determined by Mean function and Covariance functions by GaussianProcesses.jl in Julia, and hyperparameters were optimized by the GPML v4.2 code in MATLAB.

The full dataset of the residual errors was divided into a training set (CK, PP1, and PP10) and a prediction validation set (PP5 and PP20). The RSS (eq. (2)) and RMSE (eq. (3)) of the trained model were calculated between the observed accumulated methane production of PP5 and PP20, and the sum of the Gompertz model fitted results, and the Gaussian Process model predicted results.

$$RSS = \sum_{i=1}^{18} (AMP_i - (AMP(t) + GP(t)))^2 \quad (2)$$

$$\mathrm{RMSE} = \sqrt{RSS/18} \quad (3)$$

2.4. Microbial community analysis

The FastDNA Spin Kit for Soil (MP Biomedicals, USA) was used for DNA extraction from 0.2 ml of each sample. The DNA extraction was performed according to protocols of the Kit (MP Biomedicals, USA). PCR primer 515F/806R targeting 16SV4 region of bacteria was used for microbial community analysis. The samples sent to Majorbio Co. Ltd. (Shanghai, China) for small-fragment library construction and pair-end sequencing (Illumina Miseq, USA).

The pair-end data was submitted to the NCBI Sequence Read Archive (SRA) under the project number of PRJNA642168, after removing the barcode and validation. Pair-end reads from the original DNA fragments were merged using FLASH, and filtered out using UCHIME against the "gold" database, to get the clean reads. The taxonomic classification of the sequences in each sample conducted individually by Mothur, using the Ribosomal Database Project (RDP) Classifier 11.5 with a bootstrap cut off at 0.5 (Poirier et al., 2017). The operational taxonomic unit (OTU) tables and taxonomy summary files were generated after normalized by minimal sample sequence 50,998 to compare fairly.

2.5. Physicochemical analysis

The total solids (TS), volatile solids (VS), and total ammonia (TN) were determined using APHA methods. The pH was determined using an electrode (Multi 3420, WTW, Germany). Samples were centrifuged (6000 rpm, 10 min) and filtered with 0.45 μm membrane for the following tests. The ammonia and soluble chemical oxygen demand (COD) determined using DR2800 (HACH Inc., USA). Protein and polysaccharide determined by the modified Lowry method and the Dubois method, respectively. Volatile fatty acids (VFAs) were quantified by a Shimadzu GC-2010 gas chromatograph (Shimadzu Inc., Japanese), using a flame ionization detector and a Nukol free fatty acid phase (DB-FFAP) fused-silica capillary (30 m 0.32mmi.d.) GC column (Agilent Inc., CA, USA) as previously described (Yu et al., 2018).

The FAN concentration (eq. (4)) was calculated by ideal equilibria method (FAN) and modified Davis method (FAN_r), respectively (Astals et al., 2018; Capson-Tojo et al., 2020; Wangersky, 1994). The activity coefficient of monovalent ions γ equals to 1 for ideal FAN, or equals to eq. (5) for FAN_r.

$$\mathrm{FA} = \frac{\mathrm{TAN} \times K_a \times \gamma}{K_a \times \gamma + 10^{-pH}} \quad (4)$$

$$\gamma = -0.5198 \times \left(\left(\frac{\sqrt{I}}{1+\sqrt{I}} \right) - 0.20 \times I \right) \quad (5)$$

$$K_a = K_{a25} \times e^{\frac{51965}{R}\left(\frac{1}{298.15} - \frac{1}{T}\right)} \quad (6)$$

where the constant R and K_{a_25} is the ideal gas constant 8.314 J/mol/K and the acid dissociation constant $K_a = 10^{-9.25}$ at 298.15 K (25 °C), respectively. T is the temperature in kelvin (K), K_a is the dissociation constant at temperature T (eq. (6)). The I refer to media ionic strength, suggested as 0.07–0.20 M for the mixed liquid of the anaerobic digestion.

2.6. Statistical analysis

The paired-samples *t*-test was used to evaluate the significance of the differences in the methane production caused by the PPI stress during anaerobic digestion of tryptone. The random-forest machine-learning method was applied to acquire the best discriminant performance of digestion phases across the temporal evolution of the microbial community (Zhang et al., 2019). NMDS, LEfSe, Procrustes, PICRUSt, and FAPROTAX v.1.2.3 analyses were conducted on the Galaxy platform (hutten-hower.sph.harvard.edu/galaxy/).

Random-forest is a classifier contains multitude decision trees based on the threshold abundance of the critical genus. Random-forest corrects for decision trees' habit of overfitting to the microbial community by algorithm improvement, especially out-of-bag error estimation (object function) and permutation variable evaluation. These functions were all accessible by using package *randomForest* v.4.6–14 in R v.3.6.3 (Zhang et al., 2019). To acquire the best discriminant performance of the evolution of the microbial community, the abundance of bacterial taxa was classified in the phylum, class, order, family, and genus level against digestion time using the package with default parameters. All the samples (n = 15) were used as the training set and the random-forest (importance = T, proximity = T) function to generate the classification model for the evolution of the microbial community. Cross-validation was performed by the rfcv() function for selecting appropriate features, as suggested (Zhang et al., 2019). The varImpPlot() and MDSplot() function was used to show the importance of taxa and performance in classification, respectively. The function of the critical taxa was identified on the LSPN platform (lpsn.dsmz.de).

3. Results and discussion

3.1. Methane production of anaerobic digestion with PPI dose

The paired-sample *t*-test indicated that the PPI dose significantly changed the methane production kinetics in anaerobic digestion of tryptone ($p < 0.05$), by maximal 18.72 ± 7.39% at day 3 in PP20 (Fig. 1A). The daily methane production developed a gradient with PPI dose (Fig. 1B). A peak of daily methane production resurfaced at day 14, attributed to volatile fatty acids (VFAs) release on day 13 (Fig. 1C). After the first peak of daily methane production peak, PP20's VFAs were significantly lower than others ($p < 0.05$) on day 10–33. The residual

VFAs were lowest 239.77 mg/L in group PP5. Acetate accumulation observed in all groups as a potential indicator of ammonia inhibition in anaerobic digestion of tryptone (Poirier et al., 2016).

Gompertz model showed that PPI changed biochemical methane potential (BMP) and lag-phase period (Table 1). A stepwise increase of BMP was observed at PP5 and PP20, respectively. A stepwise decrease in the lag-phase period was observed at PP20. The tryptone, as a common model substrate, the lag-phase period, may not long enough to reflect obvious changes. The RSS and RMSE of the Gompertz model (Table 1) were similar to existing researches (Ware and Power, 2017), indicating similar ranges of residual errors for modeling the accumulated methane production in anaerobic digestion of tryptone with PPI dose.

The physicochemical performance indicates PPI decreased the initial accumulation of intracellular ammonia due to passive transport (diffusion) of FAN, by inhibiting proton pump from pumping extra proton to intracellular circumstance. The extracellular pH was, therefore, also lower with PPI dose (Yu et al., 2018). PPI also saved energy from proton pumping and storage the saved energy in the form of polysaccharide as a consequence of inhibition of the proton pump. The initial phase was critical in ammonia inhibition, and acclimation for many reasons. During the initial phase, more ATP energy was wasted on pumping proton intracellular for balancing intracellular pH caused by passive transport of FAN by diffusion. The preliminary results demonstrated the potential of PPI in the mitigation of initial ammonia inhibition by blocking the unwanted proton pumping. The wasted energy was reserved in intracellular storage in the form of polysaccharide and could be used for methane production in the following phases. More importantly, ammonia was less accumulated in intracellular thanks to less passive transport of FAN by blocking the unwanted proton pumping into intracellular circumstances. The less accumulation of intracellular ammonia was consistent with the observation that PP20 has a shorter lag-phase period. The performance results of tryptone as a model substrate supported further investigation of PPI's effects in anaerobic digestion of protein-rich substrates. The result also implies that PPI is promising in mitigating ammonia inhibition for anaerobic digestion of protein-rich substrate.

3.2. Residual learned by Gaussian Processes

The Gaussian Processes performed well in modeling the residual errors of the Gompertz model of the accumulated methane production in anaerobic digestion of tryptone with PPI dose (Fig. 1D&E). The trained

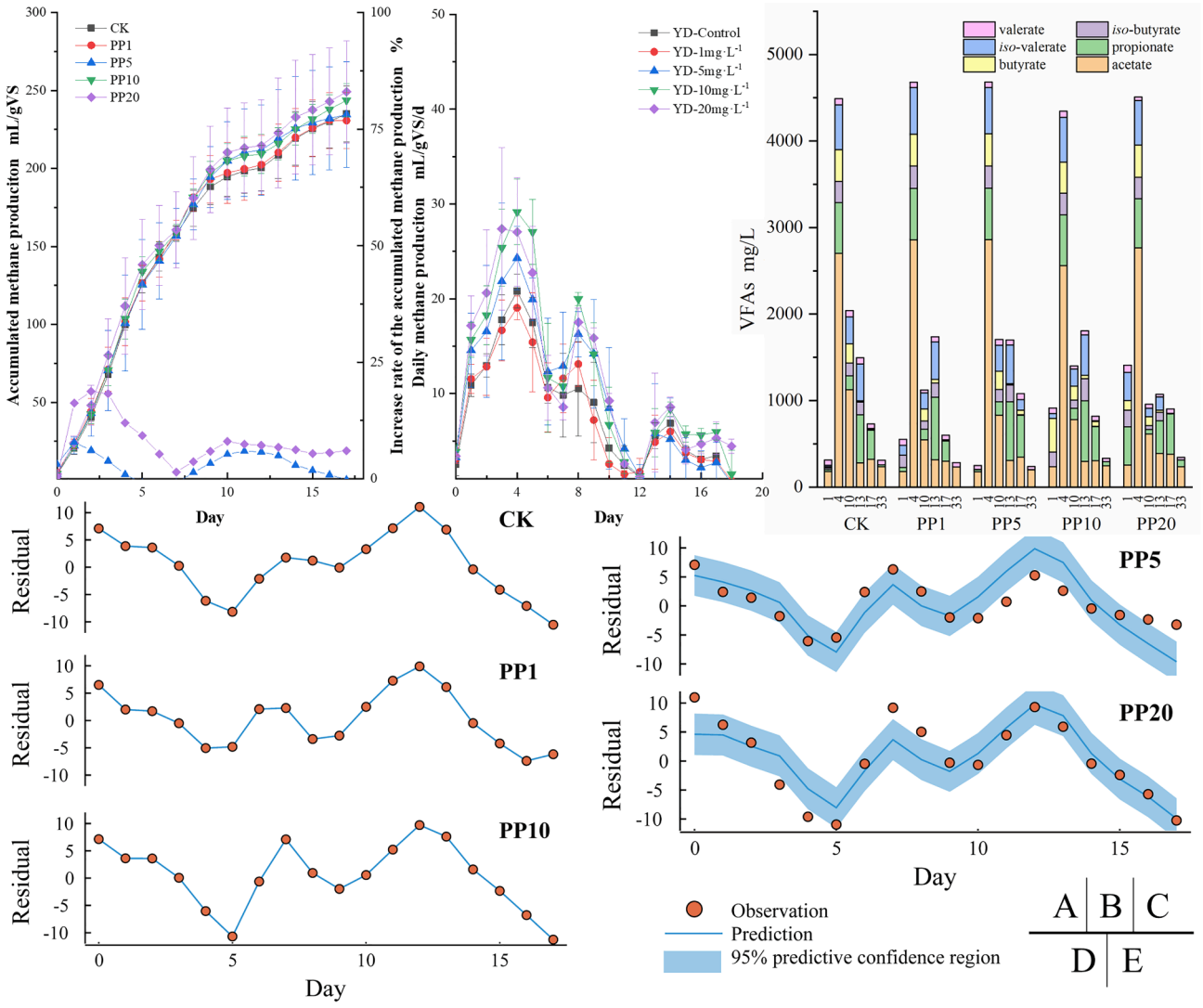

Fig. 1. Methane production and volatile fatty acids in anaerobic digestion with proton pump inhibitor dose: A) accumulated methane production and increase rate; B) daily methane production; C) volatile fatty acids (VFAs). The dose of proton pump inhibitor was control (CK), 1 mg/L (PP1), 5 mg/L (PP5), 10 mg/L (PP10), and 20 mg/L (PP20), respectively. Gaussian Processes model accurately predicts the residual of the Gompertz model of accumulated methane production. D) Group CK, PP1, and PP10 were training set. E) Group PP5 and PP20 were validation set for prediction by the trained Gaussian Processes model.

Table 1
Methanogenic kinetics of anaerobic digestion with the PPI dose. The Mean Squared Error (MSE) and Residual Sum of Squares (RSS) for kinetics and random effects model showing improved accuracy by the sum of kinetic effects and random effects.

	Gompertz model					Gaussian prediction Of the residual error of the Gompertz model	
	BMP ($mlCH_4/g$)	R_m ($mlCH_4/g/day$)	λ(day)	RSS	RMSE	RSS	RMSE
CK	228.15	0.31	0.35	601.54	6.33	1.94×10^{-11}	1.04×10^{-6}
PP1	227.86	0.31	0.30	432.84	5.37	2.84×10^{-11}	1.26×10^{-6}
PP5	235.41	0.30	0.38	241.72	4.01	194	3.28
PP10	236.31	0.31	0.35	644.40	6.55	2.57×10^{-11}	1.19×10^{-6}
PP20	243.54	0.29	0.09	794.10	7.28	170	3.07

Gaussian Processes preciously fitted with the training set. The validation set was covered by a 95% predictive confidence interval of the trained Gaussian Processes in visual inspections. The RSS and RMSE of prediction decreased over 47% in the validation set of the Gaussian Processes.

The Gaussian Processes (eq. (7)) included squared exponential kernel functions (SE), a transform by Periodic kernel function (Periodic), and a Rational Quadratic kernel function (RQ). The functions' Hyperparameters were given before training. The hyperparameters of these functions were optimized with the training set by maximum likelihood estimation. The results indicated that exponential function was critical in both kinetics and random processes, while periodic is critical in random processes. The results demonstrated that the combination of kinetics and machine learning allows for a more accurate prediction, compare with kinetics alone. Theoretically, Gaussian Processes are promising to eliminate the random error given a big enough training data, and therefore allows for a promising step towards eliminating the "true" systematic errors caused by controllable experimental conditions (Strömberg et al., 2014).

$$kernel = SE(4.0, 4.0) + Periodic(0.0, 1.0, 0.0)^{*}SE(4.0, 0.0) + RQ(0.0, 0.0, -1.0) + SE(-2.0, -2.0); \quad (7)$$

The result also implies residual errors of the Gompertz model followed learnable random patterns. The methanogenesis function of microbial community is a combination of both deterministic kinetics and stochastic processes (Zhou et al., 2014). The deterministic kinetics and stochastic processes contributed 97.63 ± 8.93% (60.83 ~ 100%, in form of Gompertz) and 2.37 ± 8.93% (-9.51 ~ 39.17%, in form of Gaussian) in accumulated methane production, respectively. The methanogenesis kinetics would determine by critical function bacteria at a niche as a professional group (Turnbaugh et al., 2007). The result of Gompertz and Gaussian process provide kinetics evidence for the microbiome theory of deterministic kinetics and stochastic processes (Xia et al., 2018).

3.3. Evolution of microbial community

The evolution of microbial community with PPI dose is shown in Fig. 2. The total operational taxonomic unit (OTU) reached highest at day 10 (D10) by maximal 761. The alpha diversity of day 10 was higher than other days for most of the PPI dose. Analysis of similarities (ANOSIM) by Bray-Curtis distance suggesting evolution was significant in anaerobic digestion with PPI dose. The clustered as three groups, where more similarities could be found between D10 and D33 than others. The difference may attribute to different function bacteria response for four phases of methane production, and their overlap (Zhu et al., 2019).

The critical bacteria, explaining differences among the groups, were identified by Linear discriminant analysis Effect Size (LEfSe, Fig. 2D). The LEfSe were applied on taxonomy from kingdom to order. The community evolved from bacteria at D1 to acetate at D33. The Clostridiales was one of the critical bacteria in D1, who was capable of syntrophic acetate oxidation (Treu et al., 2016). The Thermotogae and Methanosarcinales were identified as critical bacteria of D10 and D33, respectively. The order Methanosarcinales (e.g., *Methanosarcina*) can use hydrogen (H_2) for methane production. The concomitant dominance of Thermotogae and hydrogenotrophic methanogens was observed (Guo et al., 2014).

The dominant phylum was Firmicutes (47.1%), Bacteroidetes (27.8%), Proteobacteria (5.8%), and Thermotogae (2.6%) in total. The dominant order was Clostridiales (31.9%), Bacteroidales (23.7%), Unclassified Firmicutes (8.6%), Clostridia (4.3), and Bacteroidetes (3.5%) in total. Order *Clostridia* and most genera in *Clostridiales* were syntrophic acetate-oxidizing bacteria (SAOB) that dominated all the samples, indicating inhibition existed (Poirier et al., 2016). The *Clostridia* order increased continuously (D1: 3.9%, D10: 4.4%, vs. D33: 4.6%) in anaerobic digestion with PPI dose. Dominant genera were elected by the top thirty genera in each sample. The dominant genera were *Porphyromonadaceae* (10.7%), *Mucinivorans* (9.0%), *Tepidimicrobium* (7.4%), *Sedimentibacter* (5.5%), *Tissierella* (5.0%), and *Clostridia* (3.7%) in total, where *Tepidimicrobium* and *Clostridia* were SAOB. Porphyromonadaceae family and the *Tepidimicrobium* genus were suggested to play a critical role in the degradation of the accumulated VFAs. As long as acetate accumulated at day 3, the syntrophic acetate oxidizing bacteria dominated all the samples and sustained from D1 to D33. The dominating methanogen was *Methanosarcina* (2.1%), which use hydrogen for methane production instead of acetoclastic methanogenesis.

3.4. Critical taxa in community evolution

Next, critical taxa were identified for the best discriminant performance classifying evolution groups or digestion phases, in common with other traits, e.g., methanogenic kinetic, VFAs, and performances. A model was established to correlate the groups with mixed liquid microbiota data at the phylum, class, order, family, and genus levels. The bacterial genus showed the highest accuracy (93.3%) of classification. Ten-fold cross-validation were carried out to evaluate the importance of critical genera. The number of critical genus and decision trees was optimized to 14 and 400 by Mean Decrease Accuracy and Mean Decrease Gini. The cross-validation error curve stabilized when the 14 most relevant genus were used (Fig. 3). Thus, the 14 genera were defined as critical taxa. The 14 genera belong to eight class, where half of them (7/14) was SAOB Clostridia. Of these, four genera showed higher abundance in D1 than others; 6 genera showed higher abundance in D10 than others; 4 genera showed higher abundance in D33 than others (FDR adjusted $p < 0.05$, Fig. 3B). The higher number of genera enriched in

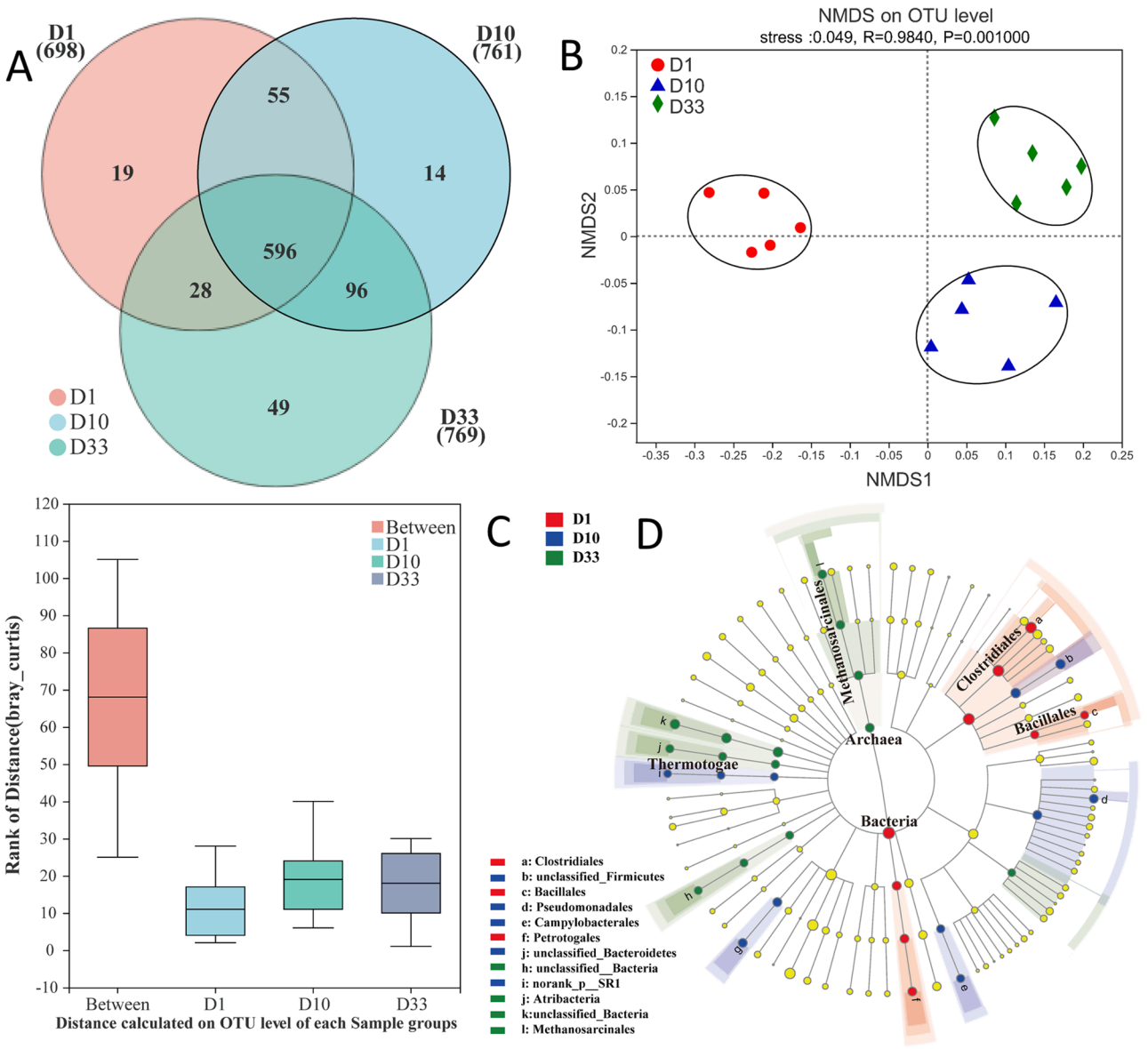

Fig. 2. Evolution of microbial community in anaerobic digestion with proton pump inhibitor dose: A) Venn diagram of the operational taxonomic unit (OUT) showing mutual taxa of different phases, B) non-metric multidimensional scaling (NMDS) on OUT level showing changes of the microbial community, C) Analysis of similarities (ANOSIM) by Bray-Curtis distance on OUT level showing the difference between phases were significant. D) LefSe analysis showing the critical taxa of different phases. Yellow dots are indicating no significant differences in abundances among the groups. (For interpretation of the references to color in this figure legend, the reader is referred to the web version of this article.)

D10 was consistent with the observation that D10 showed higher alpha diversity.

Genus *Tissierella* were fermentative acidogenic bacteria, utilizing creatinine, ammonia, monomethylamine (MMA), and carbon dioxide (Ng et al., 2015). Genus *Defluviitoga* were also acidogenic bacteria from glucose, meanwhile reduced thiosulfate and elemental sulfur, but not sulfate or sulfite, into sulfide. Genus *Clostridium* had 265 child taxa totally, over ten species detected. Some of them were also known as syntrophic oxidizing acetate to H_2 in anaerobic digestions, avoiding the accumulation of acetate under ammonia inhibition. Some of them are known to degrade complex cellulose biopolymers and lignocellulosic material components (Fitamo et al., 2017). Several *Clostridium* species producing caproic acid from short-chain fatty acids through reversed β-oxidation (Yin et al., 2017). Genus *Petrimonas* is a fermentative acidogenic bacterium, degrading protein, e.g., tryptone (Grabowski et al., 2005). To sum up, the four genera were all fermentative acidogenic bacteria, producing short-chain fatty acids in D1.

Genus *Arcobacter* can utilize the fatty and amino acids in the biological treatment facility, and some detected species able to fix nitrogen as nitrate. Genus *Pelospora* could ferment glutarate to a mixture of butyrate, *iso*-butyrate, CO_2, and acetate. Genus *Gelria* and *Tepidanaerobacter* were SAOB, which produce H_2 from acetate for hydrogenotrophic methanogenesis (Lü et al., 2014). The SAOB and genus *Methanoculleus* as hydrogenotrophic methanogens were effective in alleviating ammonia inhibition (Tian et al., 2018). To sum up, the most critical genera of D10 belongs to syntrophic methanogenic consortia (Shen et al., 2016), producing methane via syntrophic hydrogenotrophic methanogenesis pathway.

Genus *Ercella* and *Lutispora* were belonging to class Clostridia. Genus *Ercella* ferment glycerol and several carbohydrates to H_2, succinate, and acetate, where sulfur and fumarate were potential electron acceptors. The succinate was usually responsible for the yellow color of the effluent of anaerobic digestion. Genus *Lutispora* utilized tryptone and produced a mixture of acetate, *iso*-butyrate, propionate, and *iso*-valerate. Genus

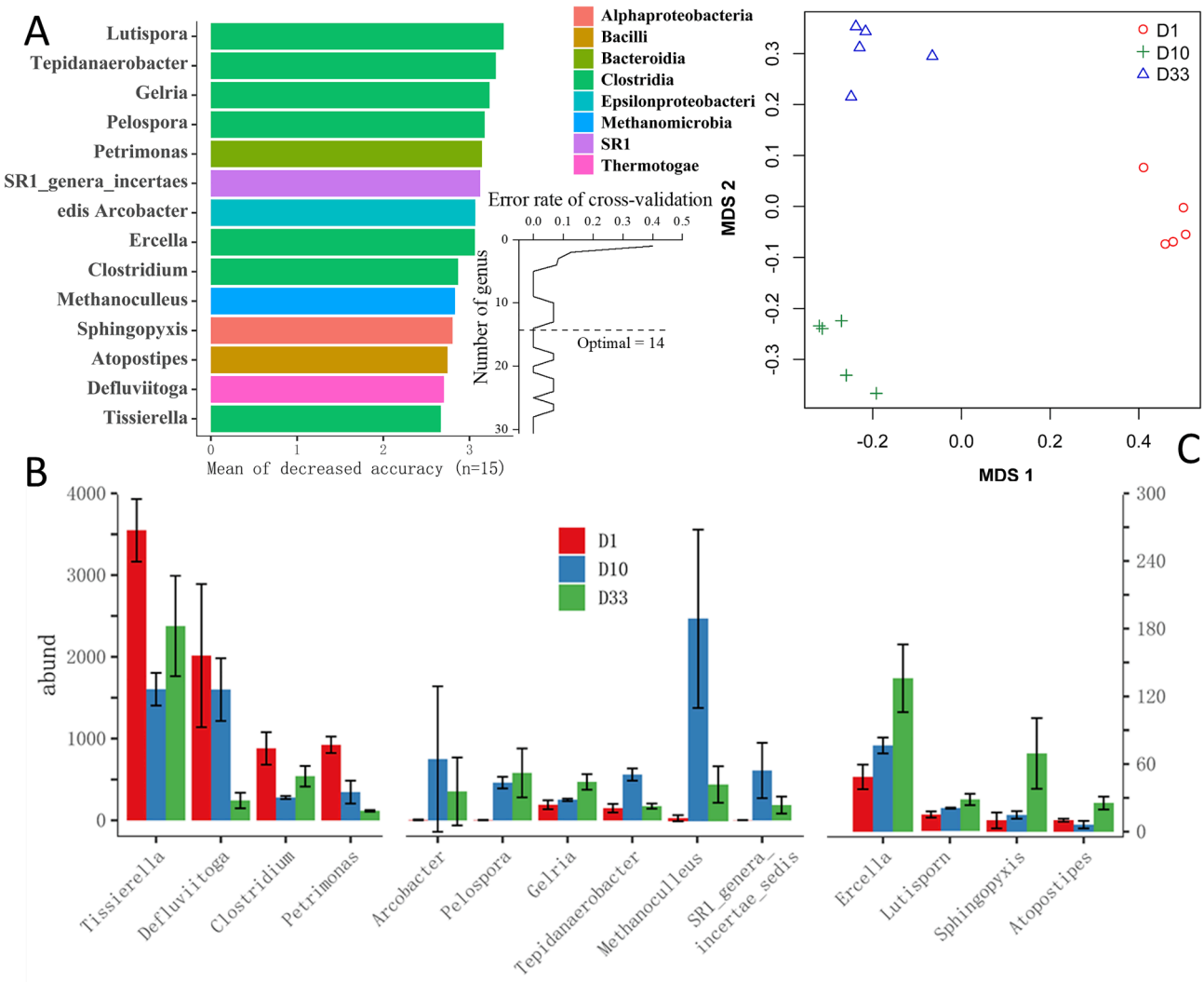

Fig. 3. Random forest model detects bacterial taxa that accurately classified different phases. A) the top 14 bacterial genera were identified by applying random-forest classification of the abundance of taxa in anaerobic digestion with PPI dose. Critical genera are ranked in descending order of importance to the accuracy of the model and colored by class. B) Critical genera with higher relative abundance in anaerobic digestion with PPI dose. Data bars and error bars represent means and standard deviation, respectively. C) Multidimensional scaling (MDS) of three phases based on the 14 critical genera showing changes of the community.

Sphingopyxis was gram-negative, producing acid from glucose, and also capable of utilizing pyruvate. Genus *Atopostipes* utilized glucose, and products of metabolism are lactate, acetate, and formate. To sum up, the four genera were all capable of producing short-chain fatty acids in D33.

3.5. Evolution of microbial functions

To explore the functional characteristics of taxa during the evolution of microbial community in anaerobic digestion with PPI dose, PICRUSt (Fig. 4A) were applied to annotate the putative function of the genus and species based on current literature (Langille et al., 2013) and the KEGG database (kegg.jp/kegg). The PICRUSt has shown its value in the metabolic function of anaerobic digestion under acute ammonia stress and should generally be used with caution (Buhlmann et al., 2019). The module M00157: F-type ATPase and M00159: V-type ATPase were inhibited at initial phase D1 with PPI dose, compared with the control CK group. The inhibited expression at PP5-D1 was consistent with the activation of PPI at the lowest pH 7.42 ± 0.04 at PP5-D1. The PICRUSt did not report the P-type ATPase. The directly targeted α subunit (H^+/K^+-exchanging ATPase subunit alpha [EC:7.2.2.19]) were associated with NADH (M00144) and NAD (M00145) module in map00190: oxidative phosphorylation (kegg.jp/kegg-bin/show_pathway? map00190), which illustrated the molecular mechanism of the proton pump. The initial inhibition (D1) of NADH (M00144) and NAD (M00115) were observed. The module M00144: NADH and M00145: NAD were inhibited at initial phase D1 with PPI dose, compare with control CK group, consistent with the inhibition of ATPase. The strongest inhibition of NADH and NAD were also observed at PP5 with lower pH active. The M00144 was linearly inhibited with an increment of PPI dose at D10 and relieved at D33 because that half-live of PPI is 1–5 day in pH > 7.1 (Shin et al., 2004). It should also be aware that NADH/NAD was widely participated in other proton transfer modules, too. There was no direct evidence here that PPI impacted interspecies hydrogen transfer, despite promising in mechanism (Tremblay et al., 2017). Similar initial inhibition (D1) and linearly inhibition with PPI dose (D10) were also observed in methane metabolism M00357: Methanogenesis, acetate to methane, and M00567: Methanogenesis, CO_2 to methane. The PPI targeted binding site in the α subunit seems highly conserved sequence (Shin and Kim, 2013) in the ATPases in anaerobic digestion (Bult et al., 1996) under ammonia stress. To sum up, the PICRUSt analysis showed the PPI dose inhibited all the three types of ATPase in anaerobic digestion under ammonia stress, directly in F-type ATPase / ATP synthase and V-type ATPase, indirectly in P-type ATPase. The module predicted by PICRUSt provide valuable insight into metabolism and how

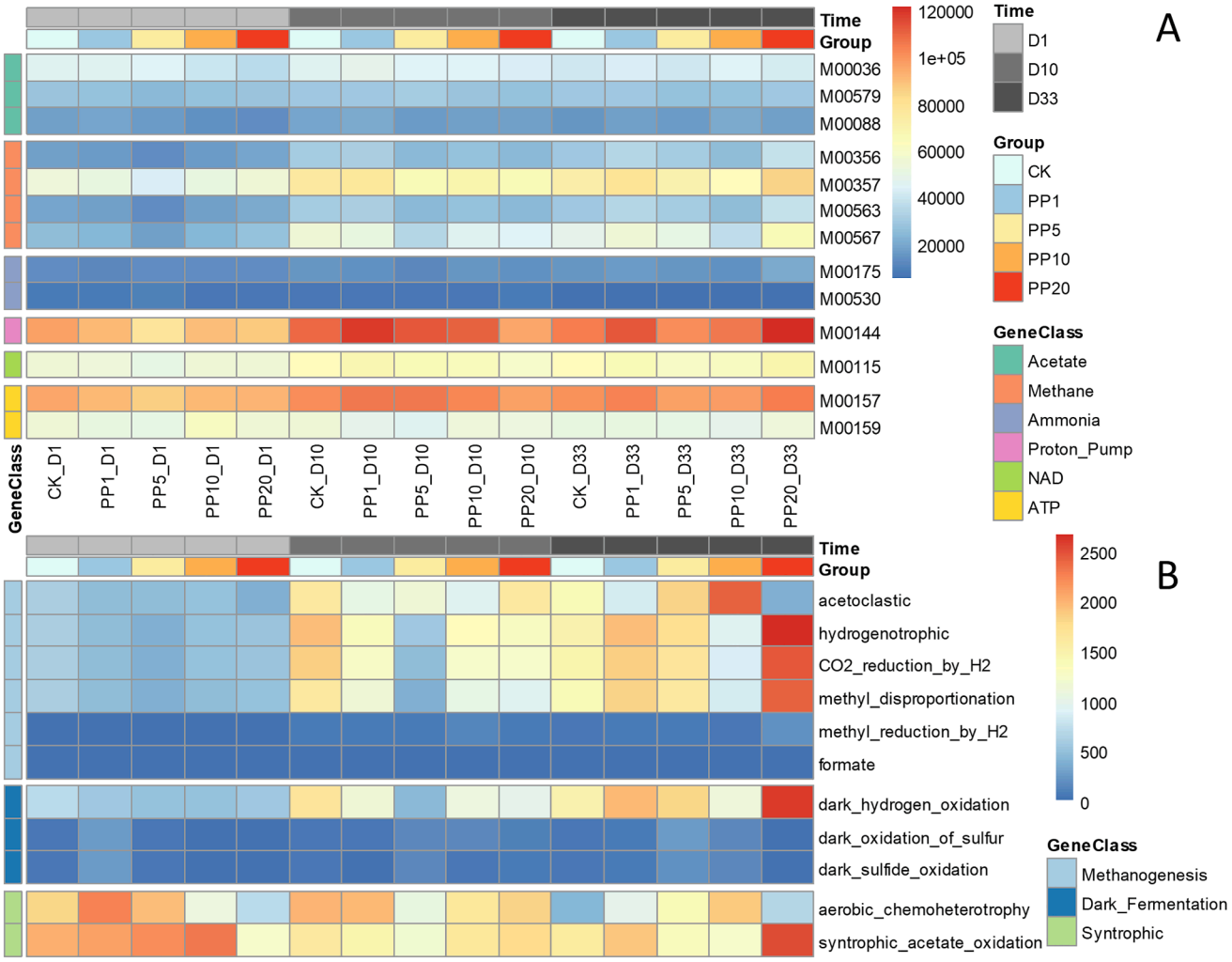

Fig. 4. Heatmap showing the evolution of function in anaerobic digestion with proton pump inhibitor dose. A) PICRUSt predicted functions in the KEGG module. GeneClass Acetate, Methane, Ammonia, Proton Pump, NAD, and ATP represented module for acetate utilization, methane metabolism, proton pump, NAD synthesize, and ATP synthesizes, respectively. B)FAPROTAX predicted function. Methane production, hydrogen production, and syntrophic metabolism-related functions were selected, showing changes in the function of the microbial community.

it shifts with PPI dose, it is promising to further investigate with metagenomic sequencing aims to all the function genes.

To further explore the functional characteristics of genus and species during the evolution of microbial community in anaerobic digestion with PPI dose, FAPROTAX (Fig. 4B) were applied to annotate the putative function of the genus and species based on current literature (Louca et al., 2016). The FAPROTAX was considered fit for function annotation in wastewater treatment (Zheng and Wen, 2019). Results showed the PPI linearly stimulated syntrophic acetate oxidation (SAO), which was the key function in acclimation to ammonia by utilizing accumulated acetate to syntrophic methanogenesis. The stimulated SAO function could sustain to D33 when PPI had been minimized. Aerobic chemoheterotrophy was also stimulated with PPI dose. Dark fermentation producing H_2 from VFAs showed similar initial inhibition (D1) and linearly inhibition with PPI dose (D10). The methanogenesis was continuously inhibited with PPI dose at D1 and D10, especially at active PP5. The hydrogenotrophic methanogenesis was more active than acetoclastic methanogenesis, except for PP5-D10, where hydrogenotrophic methanogenesis was inhibited. The hydrogenotrophic methanogenesis was stimulated by the PPI dose at D33, especially with PP20. The result is indicating that PPI dose might enhance methanogen acclimated to ammonia by initial stimulation on SAOB.

It should be noted that extra caution needed in considering the annotated function variation of archaea. The PCR primer was 515F/806R rather than 349F/806R, does not optimized for archaea. The sequencing depth of archaea was 1175 / 50,998 compared with bacteria. On the other side, the metabolism mechanism of bacteria was more reliable compare with archaea, especially for SAOB.

3.6. Critical taxa in community functions

Next, critical taxa were identified by their contribution to function using FAPROTAX, a database for converting genera into putative functional profiles based on currently cultivated strains (Zheng and Wen, 2019). The top ten function contributor was shown as Fig. 5. Of them, Genera *Clostridia, Clostridiales,* and *Methanosarcina* had identified as dominant genera in the microbial community. Genera *Clostridium*, *Petrimonas*, and *Pelospora* had identified as critical taxa in the evolution and discussed their functions in anaerobic digestion with PPI dose. Genus *Paludibacter* utilized sugars and produced propionate and acetate. Genus *Pseudomonas* is a common Gammaproteobacteria, which could utilize glucose.

The 10 genera belong to four classes, where 6/10 belongs to class Clostridia as SAOB. Genera *Sedimentibacter*, *Clostridiales*, *Clostridia*, *Clostridium*, *Pelospora*, and *Garciella* were all report SAOB. The significance of SAOB was that mitigating the accumulation of acetate caused

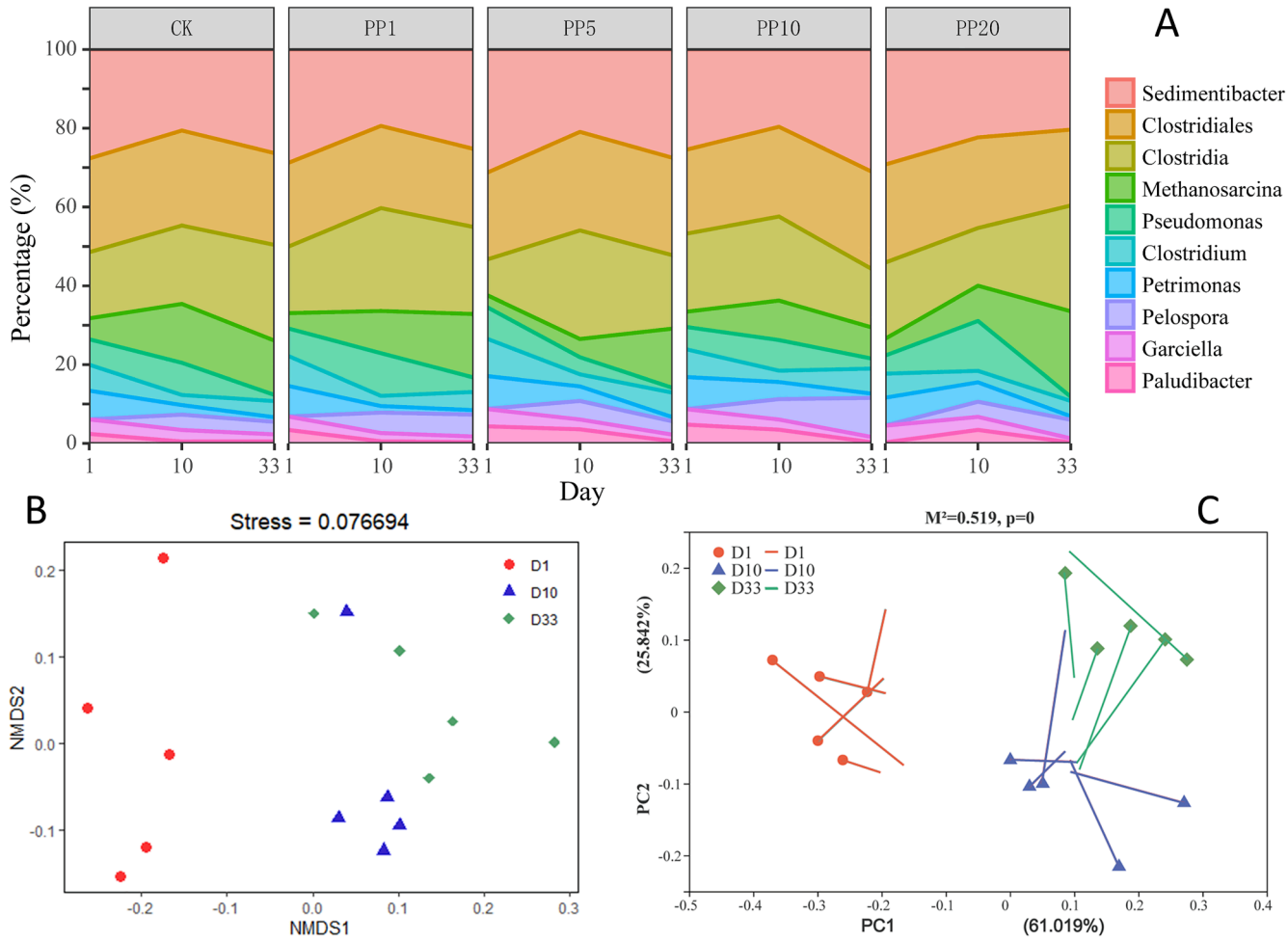

Fig. 5. Changes of Critical genera in community functions for anaerobic digestion with PPI dose. A) the top 10 genera were identified by applying FAPROTAX prediction of the performed function in anaerobic digestion with PPI dose. Critical genera are ranked in descending order of performed function using FAPROTAX. Data represent the percentage of averaged absolute abundance in each group, respectively. B) NMDS based on Bray-Curtis pairwise distances for the functions of different phases. C) Procrustes analysis based on Bray-Curtis pairwise distances for the OTU and VFAs (as intermedia metabolite) of different phases. More similarity found in function than bacteria, indicating function redundancy in the microbial community of anaerobic digestion with PPI dose.

by ammonia inhibition on methanogenesis, therefore mitigating the risk of the digestion failure due to pH drop. Although SAO was thermodynamically not preferred, it will become acceptable under ammonia stress. Most of the SAOB also syntrophic co-operate with methanogen producing CH_4, sharing the very limited energy. The bioaugmentation of anaerobic digestion by SAOB and hydrogenotrophic methanogen, was considered the most promising technology in mitigating ammonia inhibition (Fotidis et al., 2014; Tian et al., 2017; Yang et al., 2019). The PPI dose targeted SAO and stimulated SAOB as critical taxa, which is promising in case of limited availability of SAOB for a full-scale reactor.

NMDS based on function profile showed more similarity than the microbial community between D10 and D33, especially for PP5-D10, which burst into D33 cluster. The NMDS results were consistent with the function profiles by PICRUSt and FAPROTAX. The D1 phase functioned as hydrolysis, acetogenesis phase, and SAO, while the D10 and D33 phase function more as methanogenesis phase and others. The three groups were different in the NDMS1 axis, while similar in the NDMS2 axis. The Procrustes analysis was applied based on the evolution of the microbial community (OUT) and metabolism profiles (VFAs as intermediate metabolites). The Procrustes analysis confirmed more similarity in metabolism than community. The dote representing community were clustered into three groups as usual, while the line representing their intermediate metabolites had more similarity between D10 and D33. The similarity of function also profiled the redundancy of functions in the microbial community (Zheng and Wen, 2019).

3.7. *Decipher proton pump in anaerobic digestion under ammonia stress*

PICRUSt, FAPROTAX, and Procrustes analysis could provide new insight for the correlations between function and evolution of microbial community in anaerobic digestion with PPI dose. However, it cannot illustrate the detailed relationship between the specific function and microbial taxa in a visualized way. The co-occurrence between functions and microbial taxa revealed by network analysis could provide an effective complement to the overall correlation information (Luo et al., 2017).

Mantel test indicated that there existed a significant correlation between functions matrix and microbial community ($R = 0.813$, $p = 0.001$). The strong links between functions and microbial communication revealed by network analysis (Fig. 6) could aid decipher their correlations with high resolution (Luo et al., 2017). For example, methane related carbon metabolisms were strongly clustered with nitrogen metabolism in anaerobic digestion under ammonia strength. The potential mechanism was demonstrated in coupling anaerobic digestion and anammox and denitrifying anaerobic methane oxidation (DAMO) by electron transfer (Liu et al., 2019; Shi et al., 2013). The carbon metabolisms (C-metabolism) were also correlated with performances and SAOB in phylum Firmicutes suggesting SAOB as critical taxa. The SAOB

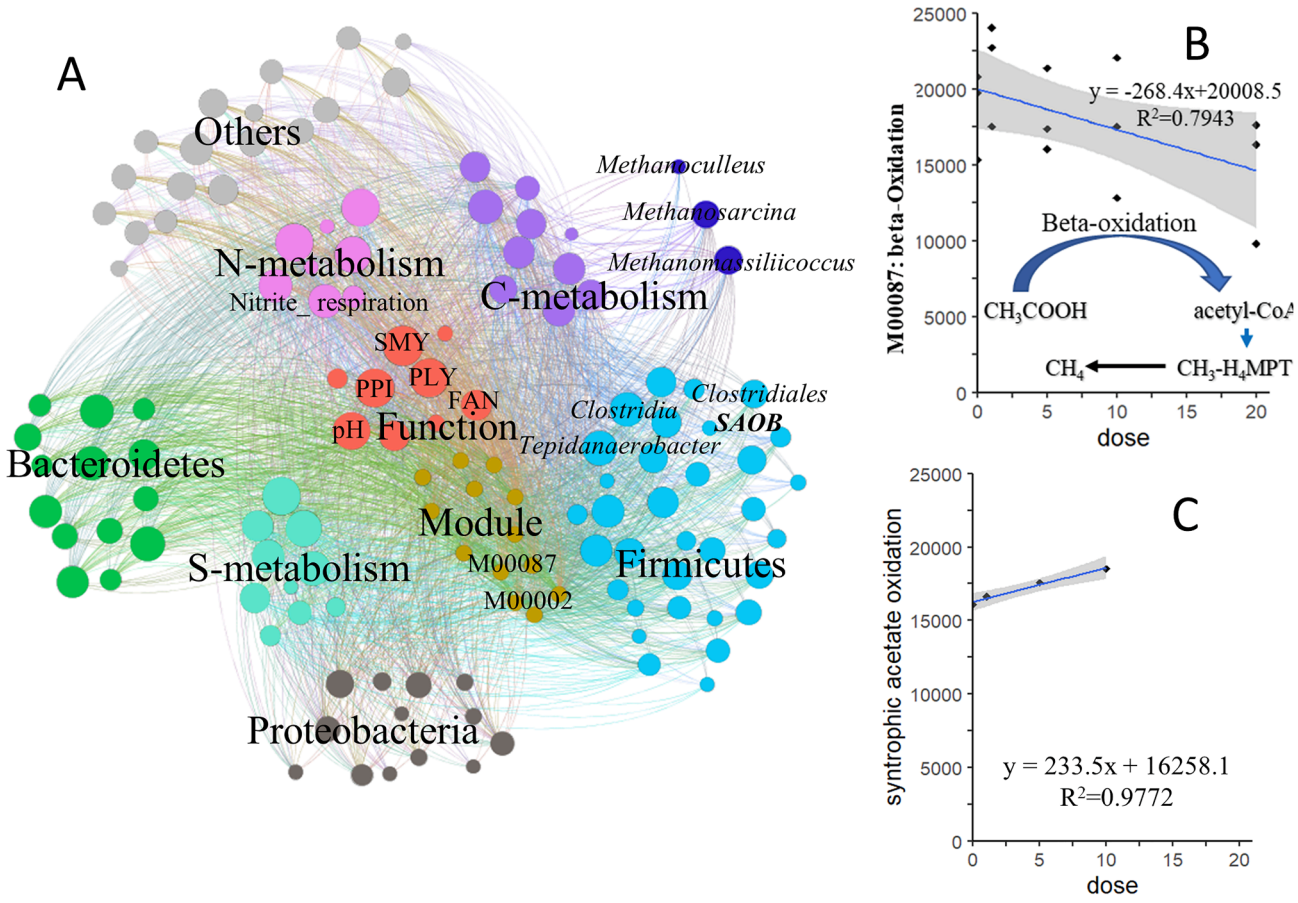

Fig. 6. Network analysis (A) based on Spearman correlation and constructed through Gephi, showing the effect of proton inhibitor on performance, functions, and bacteria. The connection indicated a significant correlation between the nodes. The connections weighted the node size. The more connections, the bigger the node size. B) Scatter with linear fit showing the relationship between the dose of proton pump inhibitor and abundance of β-oxidation, which utilize acetate to acetyl-CoA. C) Scatter with linear fit showing the relationship between the dose of proton pump inhibitor and abundance of syntrophic acetate oxidizing, which also utilize acetate to acetyl-CoA. Data of day 1 were selected when proton pump inhibitor was active judging by its reported half-life.

was used as bioaugmentation for mitigating ammonia inhibition in anaerobic digestion (Yang et al., 2019). Module, as a cluster of related functions, was strongly linked with four phyla, especially the dominant phyla Bacteroidetes and Proteobacteria. Four sequential metabolic steps are not necessarily mutually exclusive alternatives in bacteria, namely hydrolysis, acidogenesis, acetogenesis, and methanogenesis. For example, specific methane yield could linearly correlate with predicted function methanogenesis ($y = 0.10x + 28.02$, $R^2 = 0.5724$). Nevertheless, these co-operations in network analysis need further validation in further researches.

More specifically, the PPI dose was significantly related to M00087: beta-Oxidation. The overall reaction for one cycle of beta-oxidation (β-oxidation) is eq. (8) (Hagen et al., 2017).

$$C_n - acyl - CoA + FAD + NAD^+ + H_2O + CoA \rightarrow Acetyl - CoA + FADH_2 + NADH + H^+ + acyl - CoA \quad (8)$$

where fatty acid (e.g. acetate) was oxidized to fatty acyl (C_n-acyl-CoA) and acetyl-CoA (active), as a key step to methane, the correlation was accompanied with the observation that PPI stimulated SAO in FAPROTAX function results. The PPI dose was positively correlated with SAO but negatively correlated with β-oxidation (Berghuis et al., 2019). These correlations imply a possibility that the PPI target in β-oxidation, and therefore stimulated SAO as a consequence, where further investigation needed. There were two key pathways from acetate to acetyl-CoA: *ack* and *pta* via CH_3-CO-P_i for the Wood-Ljungdahl pathway, or *acs* "one-step" to acetyl-CoA for beta-oxidation (Hagen et al., 2017). These two pathways could co-occurrence in a bacteria (Treu et al., 2018) or a reactor (Buhlmann et al., 2019), and seems substitutable for each other. On the other side, their differences come along with syntrophic methanogenesis of acetate. For example, the pathways produced different ΔG_0 energy. The limited energy was shared by SAOB and syntrophic methanogens, which suggested as a key to acclimation to ammonia. There were several mechanisms describing how the energy was shared by the syntrophic methanogen consortia (Shen et al., 2016): interspecies hydrogen transfer (IHT) (Fotidis et al., 2013; Jing et al., 2017), CH_3-H_4MPT (Greening et al., 2016; Hagen et al., 2017), H_2 (Greening et al., 2016; Treu et al., 2018), and CO_2 (Zhu et al., 2019). These mechanisms could classify as interspecies electron transfer (IHT, mainly) and intermediate metabolite transfer roughly. The IHT, i.e., interspecies electron transfer via hydrogen, could also be inhibited by PPI via ATPase. In a word, the PPI dose seems regulated the acetate

metabolism in anaerobic digestion under ammonia stress, by initial inhibited ATPase / ATP synthase in the proton pump (and IHT potentially), and then triggered inhibition in β-oxidation (Hagen et al., 2017), ends up with stimulation in SAO and syntrophic methanogenesis via metabolite transfer (Zhu et al., 2019). The PPI dose has the potential to clarify these mechanisms by selective inhibition on the very first step of acetate utilization, i.e., beta-oxidation. The molecular mechanisms of ammonia acclimation would enable anaerobic digestion to recover more methane under ammonia stress.

4. Conclusions

Effects of PPI on proton pump, microbial community, and performance in anaerobic digestion under ammonia stress were investigated. The PPI inhibited abundance of ATPase genes, inhibited acetate beta-oxidation of acetoclastic methanogenesis, stimulated proton utilization for syntrophic acetate oxidizing, oriented functional evolution under ammonia stress, formed deterministic kinetics for methanogenesis, eliminated failure risk of digestion under ammonia stress. The proton pump mechanism of ammonia inhibition was refined to advance understanding of how improved methane yield and related microbial community evolution respond to ammonia stress throughout the complete process.

Author contributions

The manuscript was written through the contributions of all authors. All authors have approved the final version of the manuscript.

CRediT authorship contribution statement

Dawei Yu: Investigation, Writing - original draft, Project administration. **Qingqing Zhang:** Data curation, Investigation, Methodology. **Bram De Jaegher:** Methodology, Formal analysis. **Jibao Liu:** Data curation, Investigation, Methodology. **Qianwen Sui:** Writing - review & editing. **Xiang Zheng:** Supervision, Project administration. **Yuansong Wei:** Supervision, Project administration, Funding acquisition.

Declaration of Competing Interest

The authors declare that they have no known competing financial interests or personal relationships that could have appeared to influence the work reported in this paper.

Acknowledgments

This work was funded by the National Key Research and Development Program of China (2016YFD0501405, 2016YFE0118500), the Major Science and Technology Program for Water Pollution Control and Treatment of China (2017ZX07102-002, 2018ZX07105-001), National Natural Science Fund (21677161), and the special fund from the State Key Joint Laboratory of Environment Simulation and Pollution Control (Research Center for Eco-environmental Sciences, Chinese Academy of Sciences) (19Z02ESPCR). The author also would like to express their gratitude for Mengzi Tang from KERMIT (Knowledge-based Systems), Ghent University, for supplying valuable comments on the modeling. Dawei Yu was funded by the China Scholarship Council (CSC).

Appendix A. Supplementary data

Supplementary data to this article can be found online at https://doi.org/10.1016/j.biortech.2020.124118.

References

Astals, S., Peces, M., Batstone, D.J., Jensen, P.D., Tait, S., 2018. Characterising and modelling free ammonia and ammonium inhibition in anaerobic systems. Water Res. 143, 127–135.

Berghuis, B.A., Yu, F.B., Schulz, F., Blainey, P.C., Woyke, T., Quake, S.R., 2019. Hydrogenotrophic methanogenesis in archaeal phylum Verstraetearchaeota reveals the shared ancestry of all methanogens. Proc Natl Acad Sci USA 116 (11), 5037–5044.

Buhlmann, C.H., Mickan, B.S., Jenkins, S.N., Tait, S., Kahandawala, T.K.A., Bahri, P.A., 2019. Ammonia stress on a resilient mesophilic anaerobic inoculum: Methane production, microbial community, and putative metabolic pathways. Bioresour. Technol. 275, 70–77.

Bult, C.J., White, O., Olsen, G.J., Zhou, L., Fleischmann, R.D., Sutton, G.G., Blake, J.A., FitzGerald, L.M., Clayton, R.A., Gocayne, J.D., Kerlavage, A.R., Dougherty, B.A., Tomb, J.-F., Adams, M.D., Reich, C.I., Overbeek, R., Kirkness, E.F., Weinstock, K.G., Merrick, J.M., Glodek, A., Scott, J.L., Geoghagen, N.S.M., Weidman, J.F., Fuhrmann, J.L., Nguyen, D., Utterback, T.R., Kelley, J.M., Peterson, J.D., Sadow, P. W., Hanna, M.C., Cotton, M.D., Roberts, K.M., Hurst, M.A., Kaine, B.P., Borodovsky, M., Klenk, H.-P., Fraser, C.M., Smith, H.O., Woese, C.R., Venter, J.C., 1996. Complete Genome Sequence of the Methanogenic Archaeon, Methanococcus jannaschii. Science 273 (5278), 1058–1073.

Capson-Tojo, G., Moscoviz, R., Astals, S., Robles, Á., Steyer, J.-P., 2020. Unraveling the literature chaos around free ammonia inhibition in anaerobic digestion. Renew. Sustain. Energy Rev. 117, 109487. https://doi.org/10.1016/j.rser.2019.109487.

Fitamo, T., Treu, L., Boldrin, A., Sartori, C., Angelidaki, I., Scheutz, C., 2017. Microbial population dynamics in urban organic waste anaerobic co-digestion with mixed sludge during a change in feedstock composition and different hydraulic retention times. Water Res. 118, 261–271.

Fotidis, I.A., Karakashev, D., Kotsopoulos, T.A., Martzopoulos, G.G., Angelidaki, I., 2013. Effect of ammonium and acetate on methanogenic pathway and methanogenic community composition. FEMS Microbiol Ecol 83 (1), 38–48.

Fotidis, I.A., Wang, H., Fiedel, N.R., Luo, G., Karakashev, D.B., Angelidaki, I., 2014. Bioaugmentation as a Solution To Increase Methane Production from an Ammonia-Rich Substrate. Environ. Sci. Technol. 48 (13), 7669–7676.

Fuchs, W., Wang, X., Gabauer, W., Ortner, M., Li, Z., 2018. Tackling ammonia inhibition for efficient biogas production from chicken manure: Status and technical trends in Europe and China. Renew. Sustain. Energy Rev. 97, 186–199.

Grabowski, A., Tindall, B.J., Bardin, V., Blanchet, D., Jeanthon, C., 2005. Petrimonas sulfuriphila gen. nov., sp. nov., a mesophilic fermentative bacterium isolated from a biodegraded oil reservoir. International Journal of Systematic and Evolutionary Microbiology 55, 1113–1121.

Greening, C., Biswas, A., Carere, C.R., Jackson, C.J., Taylor, M.C., Stott, M.B., Cook, G. M., Morales, S.E., 2016. Genomic and metagenomic surveys of hydrogenase distribution indicate H2 is a widely utilised energy source for microbial growth and survival. ISME J 10 (3), 761–777.

Guo, X., Wang, C., Sun, F., Zhu, W., Wu, W., 2014. A comparison of microbial characteristics between the thermophilic and mesophilic anaerobic digesters exposed to elevated food waste loadings. Bioresour. Technol. 152, 420–428.

Hagen, L.H., Frank, J.A., Zamanzadeh, M., Eijsink, V.G.H., Pope, P.B., Horn, S.J., Arntzen, M.Ø., Liu, S.-J., 2017. Quantitative Metaproteomics Highlight the Metabolic Contributions of Uncultured Phylotypes in a Thermophilic Anaerobic Digester. Appl Environ Microbiol 83 (2). https://doi.org/10.1128/AEM.01955-16.

Jiang, Y., McAdam, E., Zhang, Y., Heaven, S., Banks, C., Longhurst, P., 2019. Ammonia inhibition and toxicity in anaerobic digestion: A critical review. J. Water Process Eng. 32, 100899. https://doi.org/10.1016/j.jwpe.2019.100899.

Jing, Y., Wan, J., Angelidaki, I., Zhang, S., Luo, G., 2017. iTRAQ quantitative proteomic analysis reveals the pathways for methanation of propionate facilitated by magnetite. Water Res. 108, 212–221.

Langille, M.G.I., Zaneveld, J., Caporaso, J.G., McDonald, D., Knights, D., Reyes, J.A., Clemente, J.C., Burkepile, D.E., Vega Thurber, R.L., Knight, R., Beiko, R.G., Huttenhower, C., 2013. Predictive functional profiling of microbial communities using 16S rRNA marker gene sequences. Nat Biotechnol 31 (9), 814–821.

Liu, T., Hu, S., Yuan, Z., Guo, J., 2019. High-level nitrogen removal by simultaneous partial nitritation, anammox and nitrite/nitrate-dependent anaerobic methane oxidation. Water Res. 166, 115057. https://doi.org/10.1016/j.watres.2019.115057.

Louca, S., Parfrey, L.W., Doebeli, M., 2016. Decoupling function and taxonomy in the global ocean microbiome. Science 353 (6305), 1272–1277.

Lü, F., Bize, A., Guillot, A., Monnet, V., Madigou, C., Chapleur, O., Mazéas, L., He, P., Bouchez, T., 2014. Metaproteomics of cellulose methanisation under thermophilic conditions reveals a surprisingly high proteolytic activity. ISME J 8 (1), 88–102.

Luo, G., Li, B., Li, L.-G., Zhang, T., Angelidaki, I., 2017. Antibiotic Resistance Genes and Correlations with Microbial Community and Metal Resistance Genes in Full-Scale Biogas Reactors As Revealed by Metagenomic Analysis. Environ. Sci. Technol. 51 (7), 4069–4080.

Mulkidjanian, A.Y., Makarova, K.S., Galperin, M.Y., Koonin, E.V., 2007. Inventing the dynamo machine: the evolution of the F-type and V-type ATPases. Nat Rev Microbiol 5 (11), 892–899.

Ng, K.K., Shi, X., Ng, H.Y., 2015. Evaluation of system performance and microbial communities of abioaugmented anaerobic membrane bioreactor treating pharmaceutical wastewater. Water Res. 81, 311–324.

Nielsen, H.B., Ahring, B.K., 2007. Effect of tryptone and ammonia on the biogas process in continously stirred tank reactors treating cattle manure. Environ. Technol. 28, 905–914.

Poirier, S., Bize, A., Bureau, C., Bouchez, T., Chapleur, O., 2016. Community shifts within anaerobic digestion microbiota facing phenol inhibition: Towards early warning microbial indicators? Water Res. 100, 296–305.
Poirier, S., Madigou, C., Bouchez, T., Chapleur, O., 2017. Improving anaerobic digestion with support media: Mitigation of ammonia inhibition and effect on microbial communities. Bioresour. Technol. 235, 229–239.
Shen, L., Zhao, Q., Wu, X., Li, X., Li, Q., Wang, Y., 2016. Interspecies electron transfer in syntrophic methanogenic consortia: From cultures to bioreactors. Renew. Sustain. Energy Rev. 54, 1358–1367.
Shi, Y., Hu, S., Lou, J., Lu, P., Keller, J., Yuan, Z., 2013. Nitrogen Removal from Wastewater by Coupling Anammox and Methane-Dependent Denitrification in a Membrane Biofilm Reactor. Environ. Sci. Technol. 47 (20), 11577–11583.
Shin, J.M., Cho, Y.M., Sachs, G., 2004. Chemistry of Covalent Inhibition of the Gastric (H + , K +)-ATPase by Proton Pump Inhibitors. J. Am. Chem. Soc. 126 (25), 7800–7811.
Shin, J.M., Kim, N., 2013. Pharmacokinetics and Pharmacodynamics of the Proton Pump Inhibitors. J Neurogastroenterol Motil 19 (1), 25–35.
Shin, J.M., Sachs, G., 2004. Differences in binding properties of two proton pump inhibitors on the gastric H+,K+-ATPase in vivo. Biochem. Pharmacol. 68 (11), 2117–2127.
Sprott, G.D., Patel, G.B., 1986. Ammonia toxicity in pure cultures of methanogenic bacteria. Syst. Appl. Microbiol. 7 (2-3), 358–363.
Strömberg, S., Nistor, M., Liu, J., 2014. Towards eliminating systematic errors caused by the experimental conditions in Biochemical Methane Potential (BMP) tests. Waste Manage. 34 (11), 1939–1948.
Tian, H., Fotidis, I.A., Mancini, E., Angelidaki, I., 2017. Different cultivation methods to acclimatise ammonia-tolerant methanogenic consortia. Bioresour. Technol. 232, 1–9.
Tian, H., Fotidis, I.A., Mancini, E., Treu, L., Mahdy, A., Ballesteros, M., González-Fernández, C., Angelidaki, I., 2018. Acclimation to extremely high ammonia levels in continuous biomethanation process and the associated microbial community dynamics. Bioresource Technology 247, 616–623.
Tremblay, P.-L., Angenent, L.T., Zhang, T., 2017. Extracellular Electron Uptake: Among Autotrophs and Mediated by Surfaces. Trends Biotechnol. 35 (4), 360–371.
Treu, L., Campanaro, S., Kougias, P.G., Sartori, C., Bassani, I., Angelidaki, I., 2018. Hydrogen-Fueled Microbial Pathways in Biogas Upgrading Systems Revealed by Genome-Centric Metagenomics. Frontiers in Microbiology 9, 1–16.
Treu, L., Campanaro, S., Kougias, P.G., Zhu, X., Angelidaki, I., 2016. Untangling the Effect of Fatty Acid Addition at Species Level Revealed Different Transcriptional Responses of the Biogas Microbial Community Members. Environ. Sci. Technol. 50 (11), 6079–6090.
Turnbaugh, P.J., Ley, R.E., Hamady, M., Fraser-Liggett, C.M., Knight, R., Gordon, J.I., 2007. The Human Microbiome Project. Nature 449 (7164), 804–810.
Wang, H., Fotidis, I.A., Angelidaki, I., Stams, A., 2015. Ammonia effect on hydrogenotrophic methanogens and syntrophic acetate-oxidizing bacteria. FEMS Microbiol. Ecol. 91 (11), fiv130. https://doi.org/10.1093/femsec/fiv130.
Wangersky, J., 1994. Principles and applications of aquatic chemistry. J. Hydrol. 155 (1-2), 293–294.
Ware, A., Power, N., 2017. Modelling methane production kinetics of complex poultry slaughterhouse wastes using sigmoidal growth functions. Renewable Energy 104, 50–59.
Wu, Y., Wang, S., Liang, D., Li, N., 2020. Conductive materials in anaerobic digestion: From mechanism to application. Bioresour. Technol. 298.
Xia, Y., Wen, X., Zhang, B., Yang, Y., 2018. Diversity and assembly patterns of activated sludge microbial communities: A review. Biotechnol. Adv. 36, 1038–1047.
Yang, Z., Wang, W., Liu, C., Zhang, R., Liu, G., 2019. Mitigation of ammonia inhibition through bioaugmentation with different microorganisms during anaerobic digestion: Selection of strains and reactor performance evaluation. Water Res. 155, 214–224.
Yin, Y., Zhang, Y., Karakashev, D.B., Wang, J., Angelidaki, I., 2017. Biological caproate production by Clostridium kluyveri from ethanol and acetate as carbon sources. Bioresour. Technol. 241, 638–644.
Yu, D., Meng, X., Liu, J., Dian, L., Sui, Q., Zhang, J., Zhong, H., Wei, Y., 2018. Formation and characteristics of a ternary pH buffer system for in-situ biogas upgrading in two-phase anaerobic membrane bioreactor treating starch wastewater. Bioresour. Technol. 269, 57–66.
Zhang, J., Liu, Y.X., Zhang, N., Hu, B., Jin, T., Xu, H., Qin, Y., Yan, P., Zhang, X., Guo, X., Hui, J., Cao, S., Wang, X., Wang, C., Wang, H., Qu, B., Fan, G., Yuan, L., Garrido-Oter, R., Chu, C., Bai, Y., 2019. NRT1.1B is associated with root microbiota composition and nitrogen use in field-grown rice. Nat. Biotechnol. 37, 676–684.
Zheng, W., Wen, X., 2019. How exogenous influent communities and environmental conditions affect activated sludge communities in the membrane bioreactor of a wastewater treatment plant. Sci. Total Environ. 692, 622–630.
Zhou, J., Deng, Y., Zhang, P., Xue, K., Liang, Y., Van Nostrand, J.D., Yang, Y., He, Z., Wu, L., Stahl, D.A., Hazen, T.C., Tiedje, J.M., Arkin, A.P., 2014. Stochasticity, succession, and environmental perturbations in a fluidic ecosystem. Proc. Natl. Acad. Sci. U.S.A. 111, E836–E845.
Zhu, X., Campanaro, S., Treu, L., Kougias, P.G., Angelidaki, I., 2019. Novel ecological insights and functional roles during anaerobic digestion of saccharides unveiled by genome-centric metagenomics. Water Res. 151, 271–279.